6. ANKARA INTERNATIONAL AEROSPACE CONFERENCE **AIAC-2011-024**
14-16 September 2011 - METU, Ankara TURKEY

ANALYSIS OF HELICOPTER FLOW FIELDS IN FORWARD FLIGHT INCLUDING THERMAL EFFECTS OF EXHAUST GASES

Zeynep Ece GÜRSOY[1] and Uğur ETİZ[2]
ASELSAN AŞ
Ankara, TURKEY

Yusuf ÖZYÖRÜK[3]
Middle East Technical University
Ankara, TURKEY

ABSTRACT

In this paper, the flow field of a utility helicopter in forward flight is investigated numerically. The study focuses particularly on the temperature distribution around the tail boom. This is done by introducing the hot engine exhaust flow into the computational domain by proper exhaust exit conditions. The commercial computational fluid dynamics software ANSYS Fluent is used for the analyses. The rotors are simulated by a Virtual Blade Model code coupled to the Fluent flow solver. Various forward flight conditions are investigated. In each case, the temperature distribution around the tail boom is compared with the available flight test data.

INTRODUCTION

Helicopter flow fields feature complex aerodynamic characteristics mainly due to the existence of rotors and interactions between main rotor wake, fuselage, tail rotor wake, and engine plume. The levels of these interactions vary depending on the flight configuration and aerodynamic loading. For example, while in some conditions the emerging hot exhaust gases do not result in important heating effects on the tail boom, in some others the hot gases graze the tail boom quite strongly resulting in excessive heating there. The problem outlined by this example is exactly what the present paper is dealing with. The heating effects of exhaust hot gases on the tail boom of a utility helicopter are solved numerically by modeling the helicopter fuselage, main and tail rotors, and the engine exhaust effects through computational fluid dynamics (CFD). The study concentrates on the temperature distribution upon the tail boom in various forward flight conditions. These temperature distributions obtained by the CFD analyses are compared to the available flight test data.

The helicopter investigated in this study is a twin-engine, medium lift, utility helicopter. During the flight tests two different pieces of equipment were mounted upstream of the tail boom on the left and right sides. These stores are included in the computational model as well.

METHOD

For the CFD computations, the commercial CFD software ANSYS Fluent [3] is utilized. Analyses are carried out using the pressure based solver. The second order upwind scheme with PRESTO! (for pressure) are used for discretization.

Modeling of the Rotors

The main and tail rotors are modeled using a Virtual Blade Model (VBM) [4], a user-defined function of Fluent. VBM is coupled with the flow field equations of Fluent's Navier Stokes solvers. Therefore, the mutual aerodynamic interaction between rotors and airframe is solved.

[1] Expert Engineer, zegursoy@aselsan.com.tr
[2] Senior Lead Design Engineer, etiz@aselsan.com.tr
[3] Professor in Aerospace Engineering, yusuf@ae.metu.edu.tr

In this user defined function, the rotors are modeled as cylindrical fluid zones. The blades are not included explicitly in the computational grid. The time-averaged effects of the rotor are modeled using source terms in the momentum equations located in a disk volume. The blade source terms develop as a part of the solution by the use of Blade Element Theory [5]. Spanwise variations for the chord length, airfoil type, and twist are allowed in VBM. The VBM also contains a trimming routine.

The realizable k- ε model is employed for this study as it has been assessed as a proper model based on the study carried out on the ROBIN geometry using the VBM and different turbulence models available in Fluent [1].

Modeling the Engine Effects

The engine exhaust effects are included in the analyses through boundary conditions. The "mass flow inlet" boundary condition of Fluent is used for both the inlets and exhausts. The mass flow rate at the inlet is calculated utilizing available engine test data and the studies of Ballin [6] and Çalışkan [2]. In Reference [6], the corrected mass flow rate at the compressor inlet versus the compressor static pressure ratio for different corrected compressor/gas generator speed is given. In order to use this chart, the engine torque values corresponding to the flight speeds are obtained using the TRIM-CF code developed by Çalışkan [2]. Then, the compressor pressure ratio and corrected gas generator speeds are obtained versus engine torque from the available engine test data. The inlet total temperature is taken to be that of the free-stream. The flow direction is taken normal to the exhaust boundary face.

For the exhaust boundary condition, the exhaust gases are approximated as hot air. Since the mass flow rate of fuel is negligible compared to that of air, the mass flow rate at the exhaust is taken equal to that at the inlet. Temperature is assumed to be uniform throughout the exhaust exit section. The exhaust gas temperature is determined using the available flight test data. The temperature at the turbine exit (TGT) is recorded during the flight test. Then, a separate ground test is carried out to measure the exhaust temperature. The temperature at the center of exhaust is measured using a thermocouple while the TGT is also recorded. The difference between the two values is added to the TGT values of the flight cases to obtain the temperatures at the exhaust.

Computational Model

An unstructured computational grid is employed. The fuselage surface grid in the tail boom region is presented in Figure 1. In order to use the Virtual Blade Model, the main and tail rotor fluid zones are modeled as two separate fluid domains within the global flow domain. Pave and Cooper schemes are used for the rotor surface and volume meshes, respectively (Figure 2).

For each advance ratio, the fuselage pitch angle and the tip path plane angle of the main rotor are different. The advance ratio μ is defined as

$$\mu = \frac{V_\infty}{\Omega R} \tag{1}$$

where V_∞ is the forward flight velocity, Ω is the angular speed of the main rotor and R is the radius of the main rotor. Therefore, a different computational grid is generated for each analysis. The fuselage pitch and tip path plane angles are obtained from the study of Çalışkan [2].

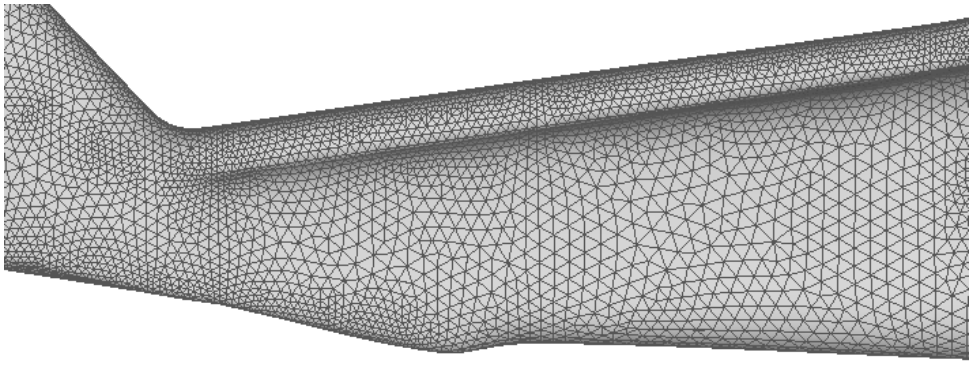

Figure 1- *Fuselage surface grid- tail boom*

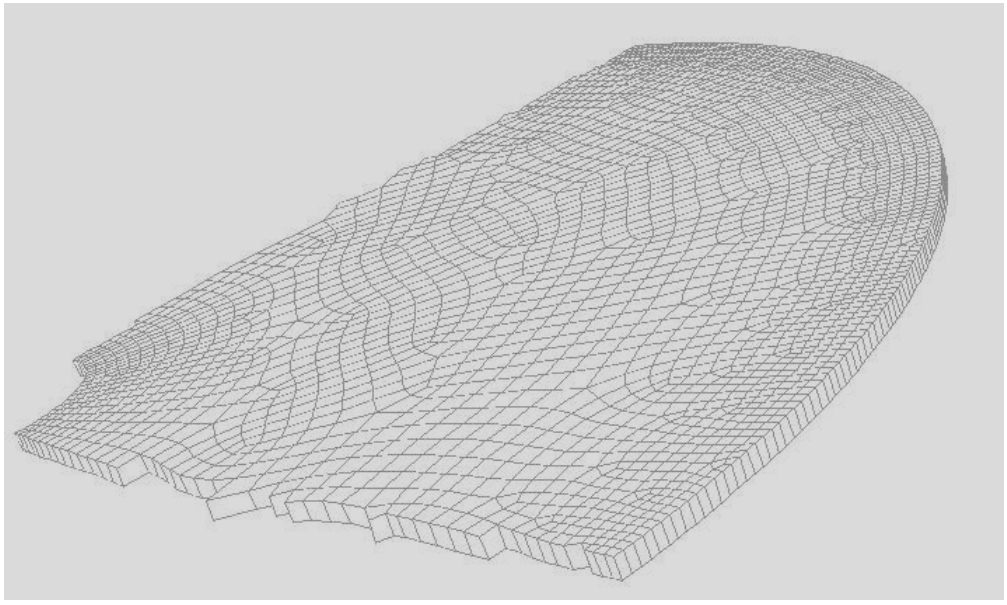

Figure 2 – *Volume mesh of fluid zone representing the main rotor in VBM - cut-out view*

UTILIZATION OF THE FLIGHT TEST DATA

In this study, for each advance ratio, the temperature distribution around the tail boom is compared with the temperature data obtained from a flight test. In the flight test, an 80-minute flight profile that consists of different advance ratio phases is performed while temperature data at 70 positions on the helicopter are recorded. In this study, the data from 36 of these points which lie around the tail boom are used.

In the tests, thermocouples are attached to the tips of 0.15 m rods which are fixed perpendicularly to the tail boom surface along four different lines on the right upper, right lower, left upper, and left lower sides of the tail boom, as shown schematically in Figure 3. The duration of the test phases changes from 27 seconds to 110 seconds, as summarized in Table 1. The data is collected by two data acquisition systems with 45 channels with a sampling rate of 4 Hz.

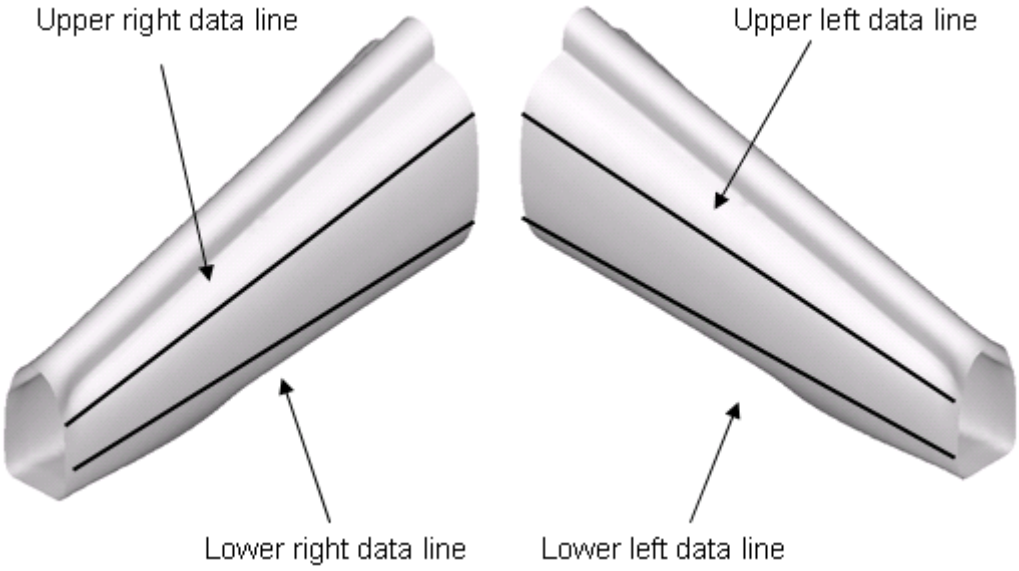

Figure 3 – *Flight test data lines on the tail boom. The data points lie along the lines shown.*

Table 1 – *Durations of the flight test phases used in this study*

Flight Phase	Duration (min: sec)
μ= 0.07	00:27
μ= 0.14	01:16
μ= 0.19	00:51
μ= 0.28	01:00

The data collected at one of thermocouple positions are shown in Figure 4. Before comparison with the CFD results, the temperature data which show sudden increases or decreases are eliminated and then an averaging procedure is applied. In Figure 5, the raw data and the corresponding averaged data are shown.

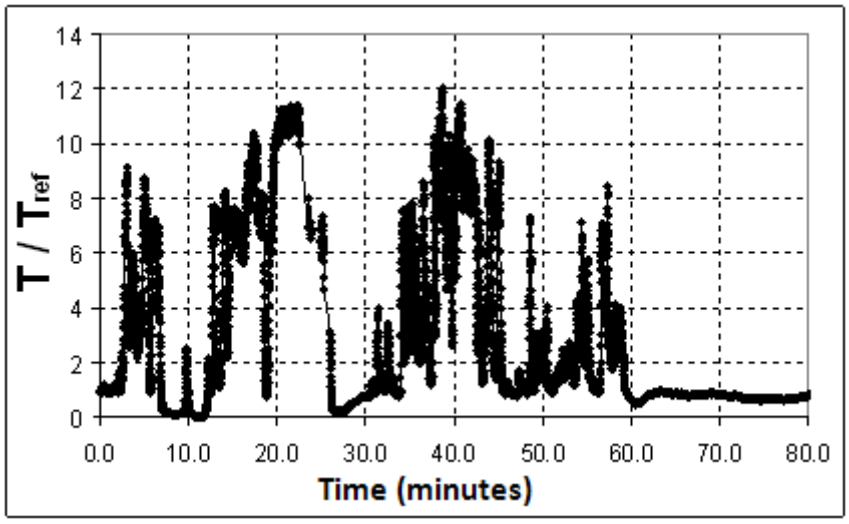

Figure 4 – *Data collected at one thermocouple during the flight tests*

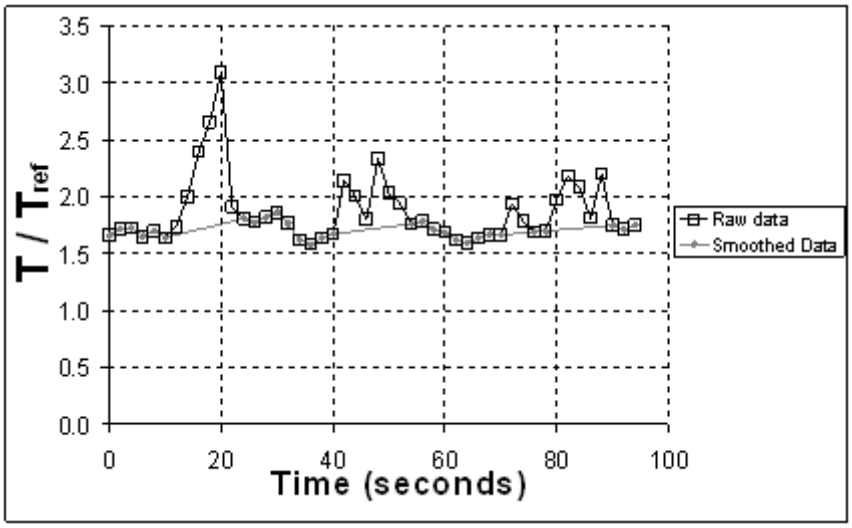

Figure 5 – *Data collected at one thermocouple at one phase: raw data and smoothed data*

RESULTS

Four forward flight cases with advance ratios of μ=0.28, μ=0.19, μ=0.14, μ=0.07 are investigated but the results for μ=0.28 and μ=0.07 are presented here. The flow fields are examined and temperatures around the tail boom are compared to the flight test data. The temperature values are extracted from the computed flow fields at 0.15 m distance off the tail boom wall, along the lines of thermocouple locations shown in Figure 3.

Forward Flight at μ=0.28

At this advance ratio, the effect of the forward flight velocity is clearly observed. Figure 6 shows the main rotor streamlines. The rotor wake is dragged downstream and it washes the rear parts of the fuselage. It interacts with the vertical and horizontal tail and the tail rotor as shown in Figure 7.

The flow that hits the stores is deflected upwards toward the exhaust jet and is heated before reaching the tail boom. Therefore, the temperature of the upper part of the boom is increased further.

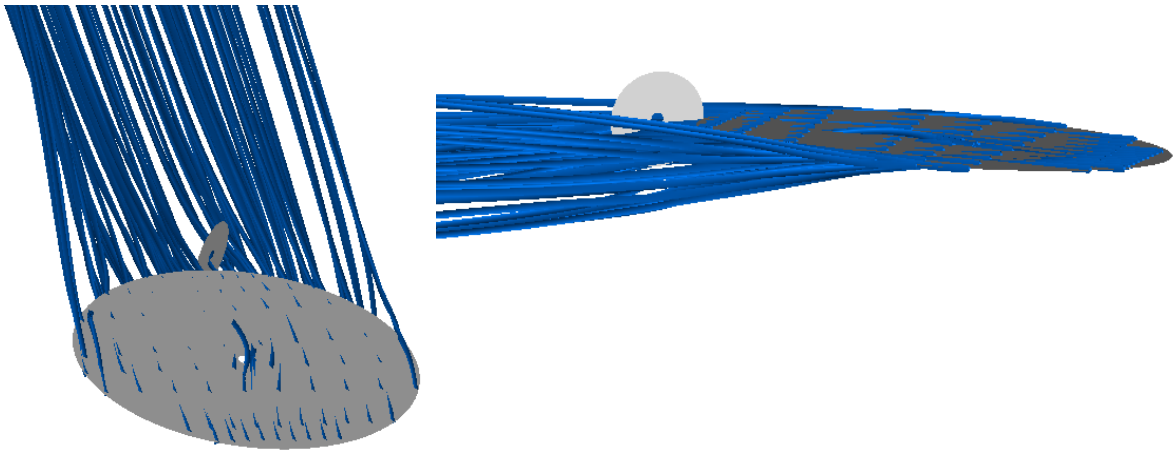

Figure 6 – *Main rotor streamlines at μ=0.28*

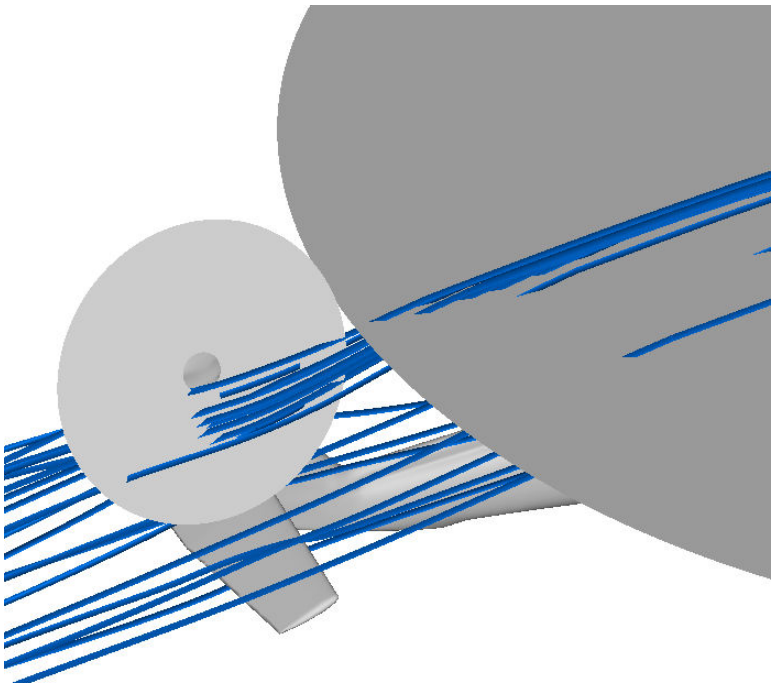

Figure 7 – *Main rotor - tail rotor, main rotor –vertical and horizontal tail interactions at μ=0.28*

Due to the interaction of the rotor wake with the exhaust gases, on the right side the exhaust comes closer to the tail boom heating that region more than that on the left side as seen in the temperature coloured streamline pattern in Figure 8. The rear upper region of the tail is affected by the hot flow due to the high forward flight velocity.

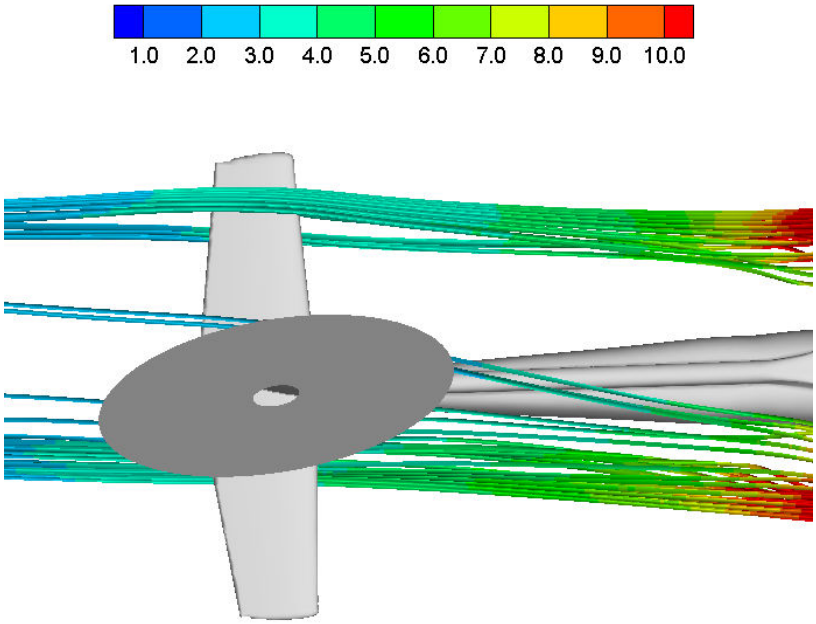

Figure 8 – *Exhaust streamlines at μ=0.28 (colored by temperature: T/Tref)*

The temperature iso-surfaces from the computed flow field are presented in Figure 9. The iso-surfaces show how the exhaust jet gets diffused and convected. Temperature plots are shown in Figure 10. The lower regions of the tail boom get heated only slightly by the exhaust jet, due to high forward flight velocity.

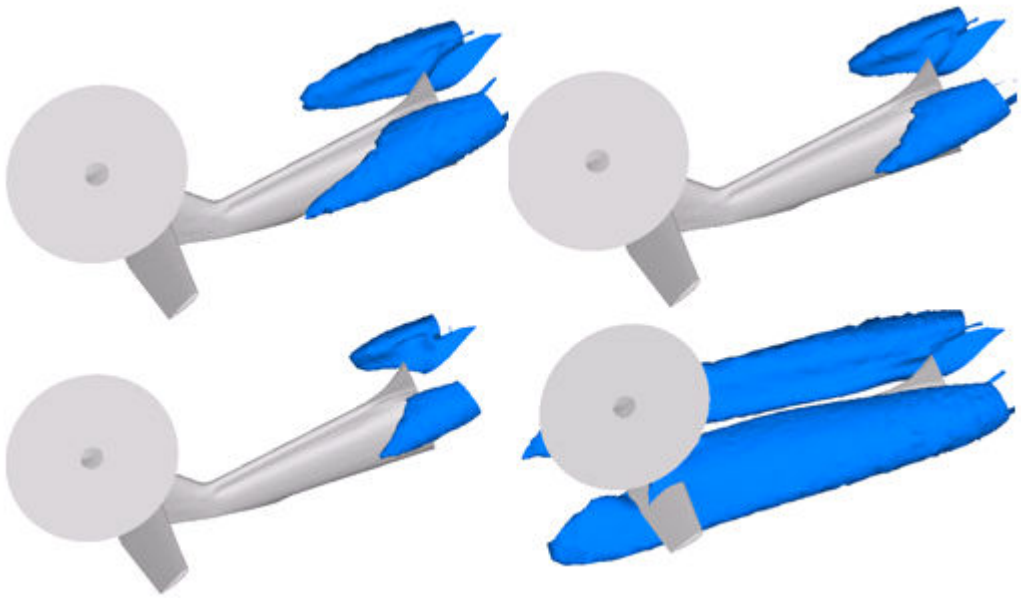

Figure 9 – *Temperature iso-surfaces at μ=0.28*

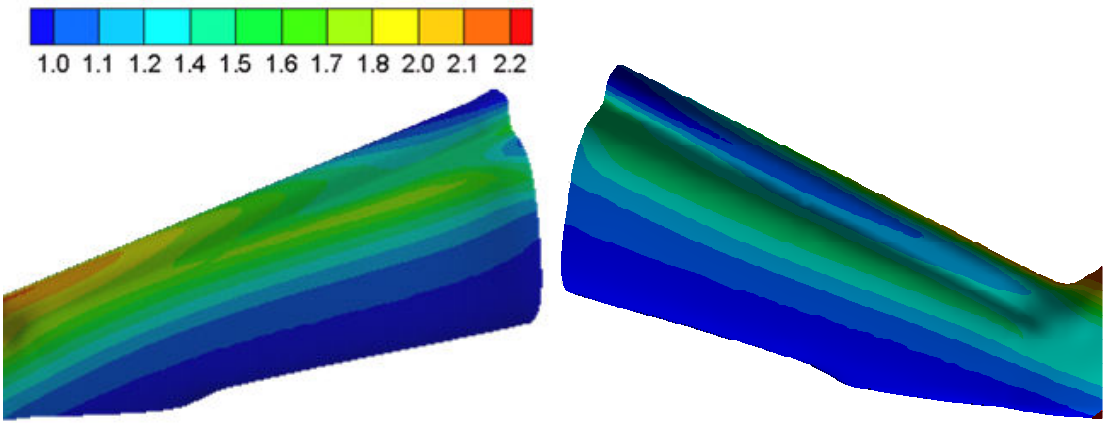

Figure 10 – *Temperature distribution on the tail boom at μ=0.28- right and left sides respectively*

Shown in Figure 11 and Figure 12 are the temperature values around the right side of the tail boom with the flight test data. The exhaust exit plane corresponds to the axial station x/L_{ref}= 0.21. The trends agree with those of the flight test data on the upper right side (Figure 11). On this data line, the values are slightly overestimated, though they are still close to the test data. The increase in temperature after about x/L_{ref}=0.32 is caused mainly the store wake. Exhaust flow comes closer to the tail boom surface. The temperature increase is overpredicted by the CFD solution and the difference between flight test data and CFD solution is not exactly constant. This behavior may be attributed to the diffusion process that the jet experiences. The store wakes interact with the exhaust jet as well.

On the lower right side, the temperature is close to the free-stream temperature upstream of the x/L_{ref}=0.47 for both the test data and the CFD solution as shown in Figure 12. Downstream of x/L_{ref}=0.47 has increasing temperature. Some hot spots on the tail were captured by the numerical solution but they were somewhat underpredicted in comparison to the measured data.

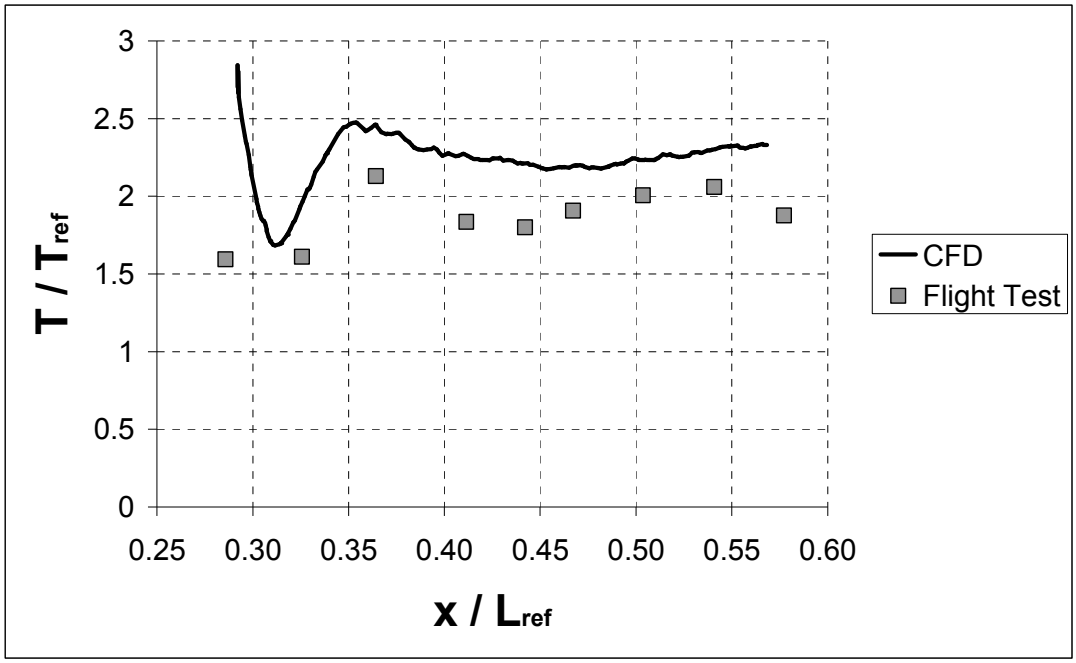

Figure 11 – *Temperature values along the upper right data line at μ=0.28*

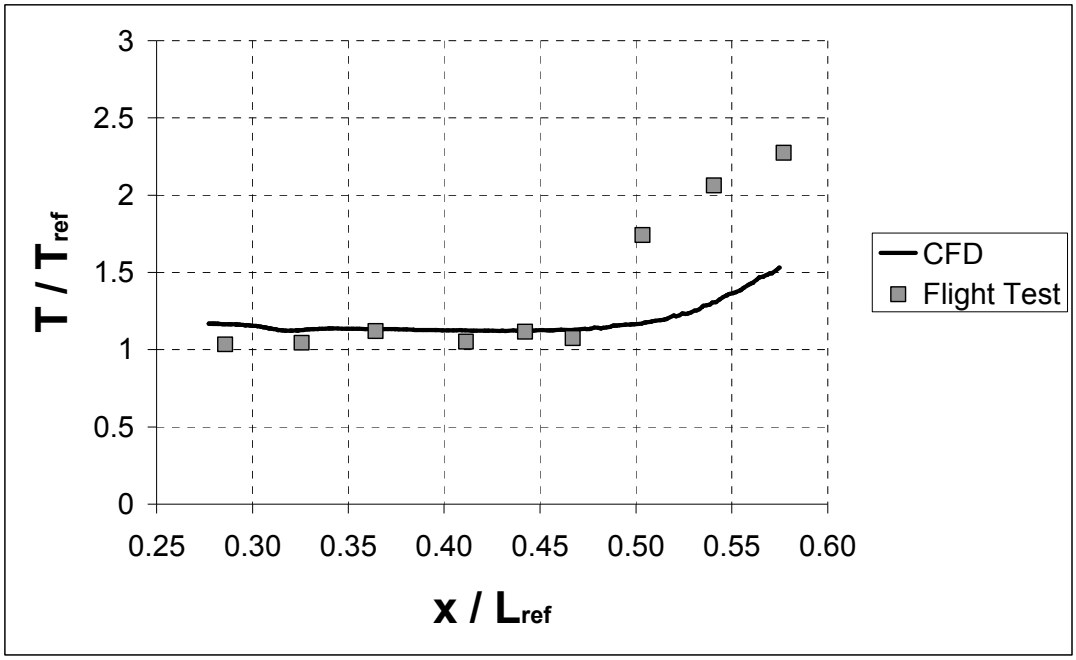

Figure 12 – *Temperature values along the lower right data line at μ=0.28*

Figure 13 shows that, to an extensive part on the upper left side, the temperature distribution is overestimated by the CFD simulation. The store wake affects this side, and the flight test data shows only some minor heating is caused by the stores at about x/L_{ref}=0.4 on the upper side. However, the test data demonstrates that the lower left side is not heated at all which is also agreed by the computations (Figure 14).

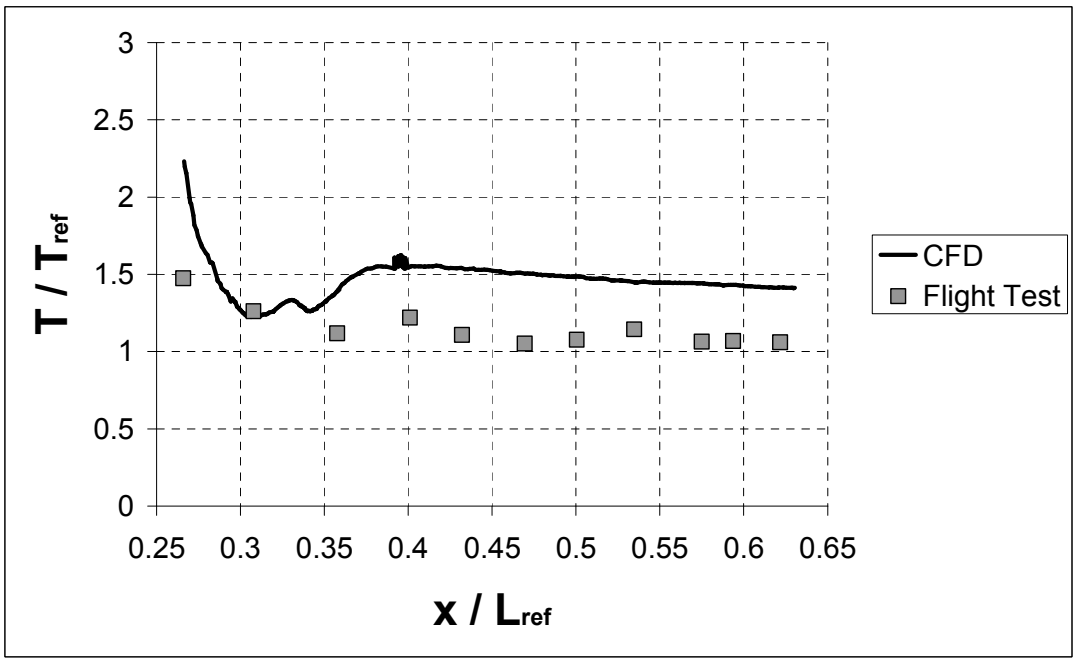

Figure 13 – *Temperature values along the upper left data line at μ=0.28*

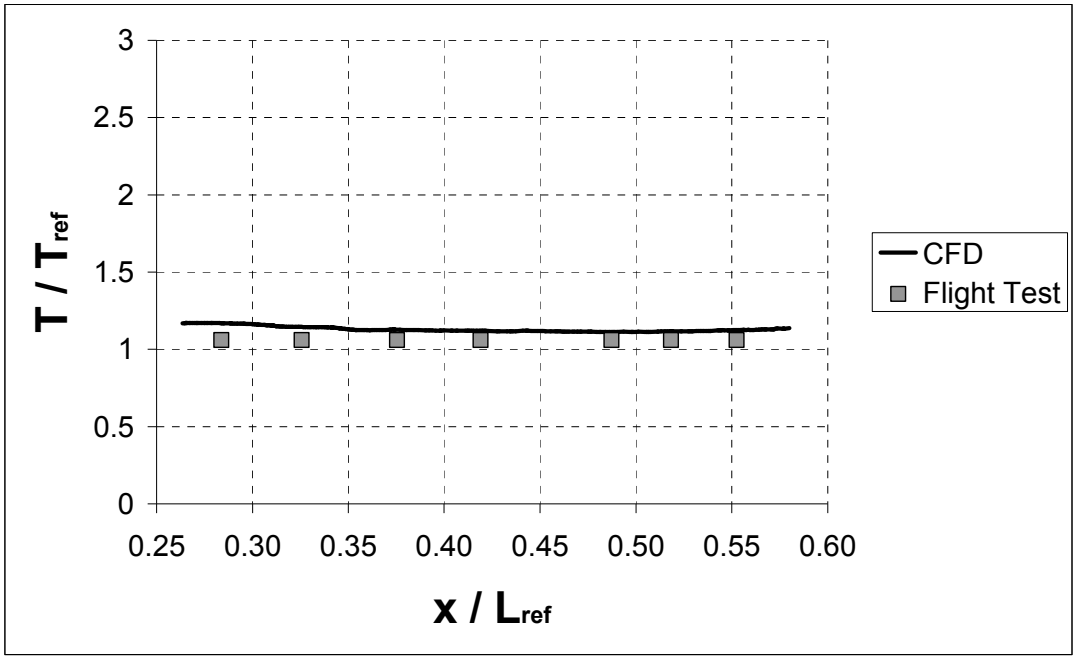

Figure 14 – *Temperature values along the lower left data line at μ=0.28*

The CFD analysis is successful in capturing the general behavior of the flow though it overestimates the temperature values in some parts. One potential reason is the assumption of uniform temperature distribution on the exhaust face and the approach used in the calculation of the exhaust gas temperature. Another reason is attributed to the possibility on atmospheric disturbances. The rough modeling of the stores is another possible reason for the temperature overestimation.

Forward Flight at μ=0.07

The main rotor wake in the flow field is dominant at an advance ratio of 0.07 as it is a low speed flight. The rotor wake has stronger tip vortices as seen in Figure 15. The flow is pushed down towards the fuselage as it sheds downstream with the effect of the forward flight velocity. The exhaust jet is strongly influenced by the main rotor downwash. It is pushed downward, heating up only the upstream parts of the tail boom as evident from both Figure 16 and Figure 17. The left exhaust approaches to the fuselage more than the right one does.

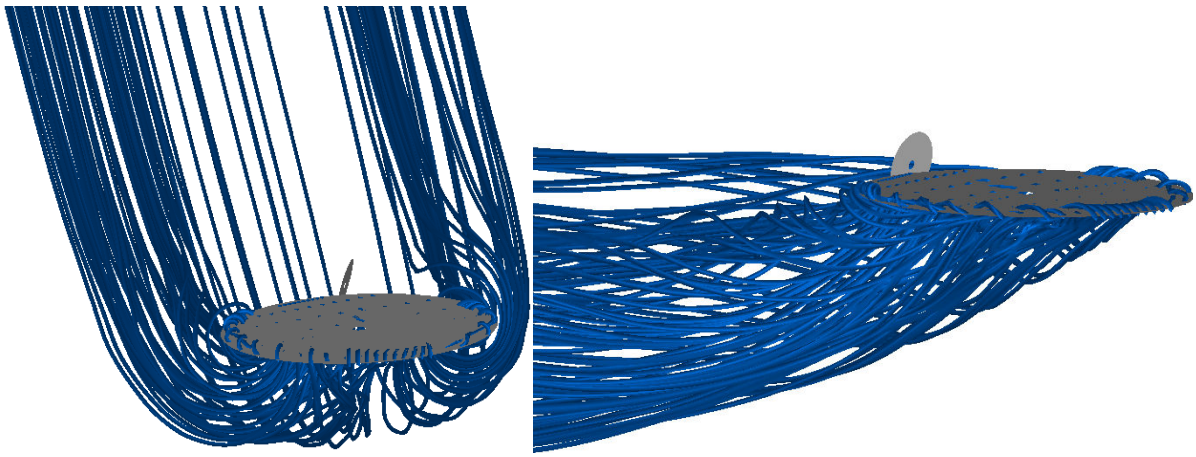

Figure 15 – *Main rotor streamlines at μ=0.07*

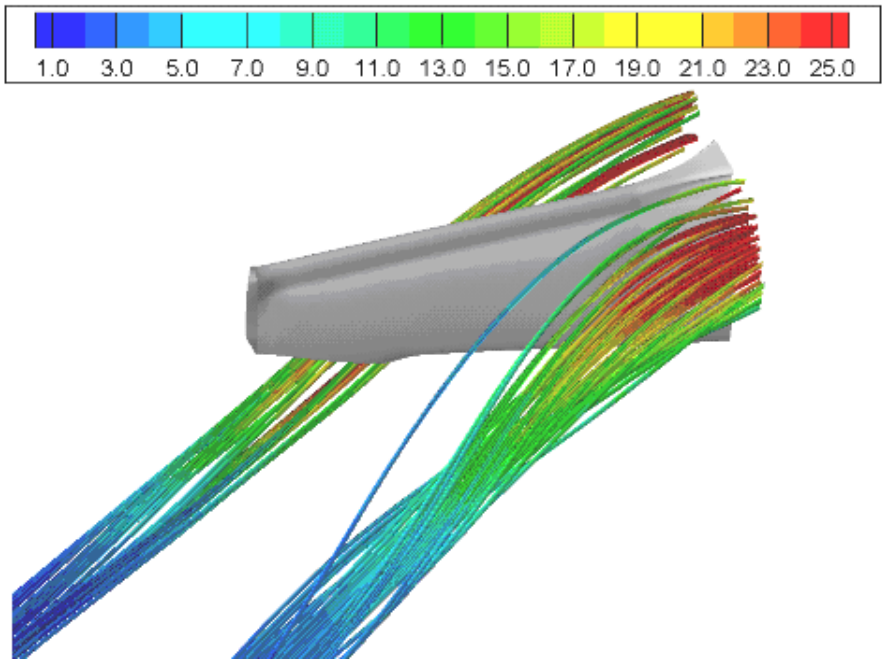

Figure 16 – *Exhaust streamlines at μ=0.07 (colored by temperature: T/Tref)*

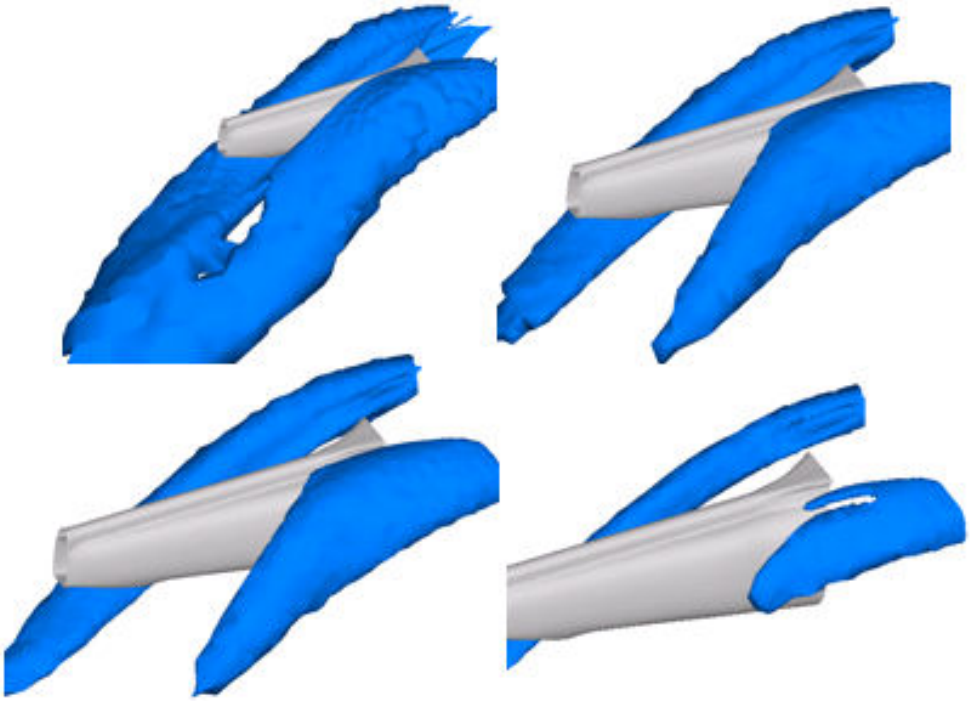

Figure 17 – *Temperature iso-surfaces at μ=0.07*

The hot flow on the left side heats the front part of the tail boom. The hot flow on the right side is dragged downstream at a higher rate and relatively farther from the surface heating this side less (Figure 18).

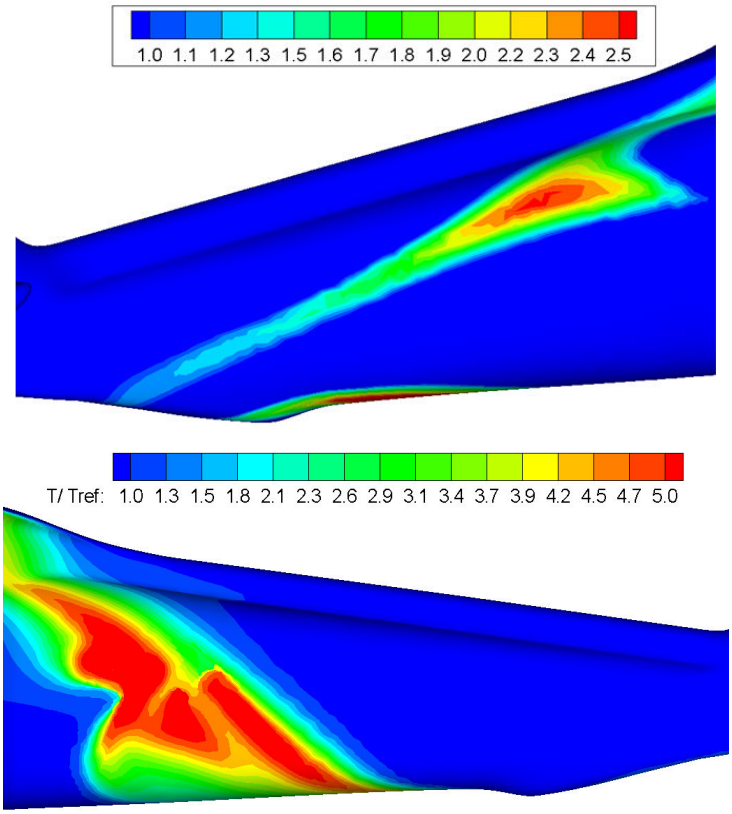

Figure 18 – *Temperature distribution on the tail boom at μ=0.07- right and left sides respectively*

Temperature distributions along the right side data lines show similar trends to those of the flight test. On the upper right side, the CFD simulations show no influence of the hot flow downstream of about the x/Lref=0.45 station, contrary to the flight test data (Figure 19).

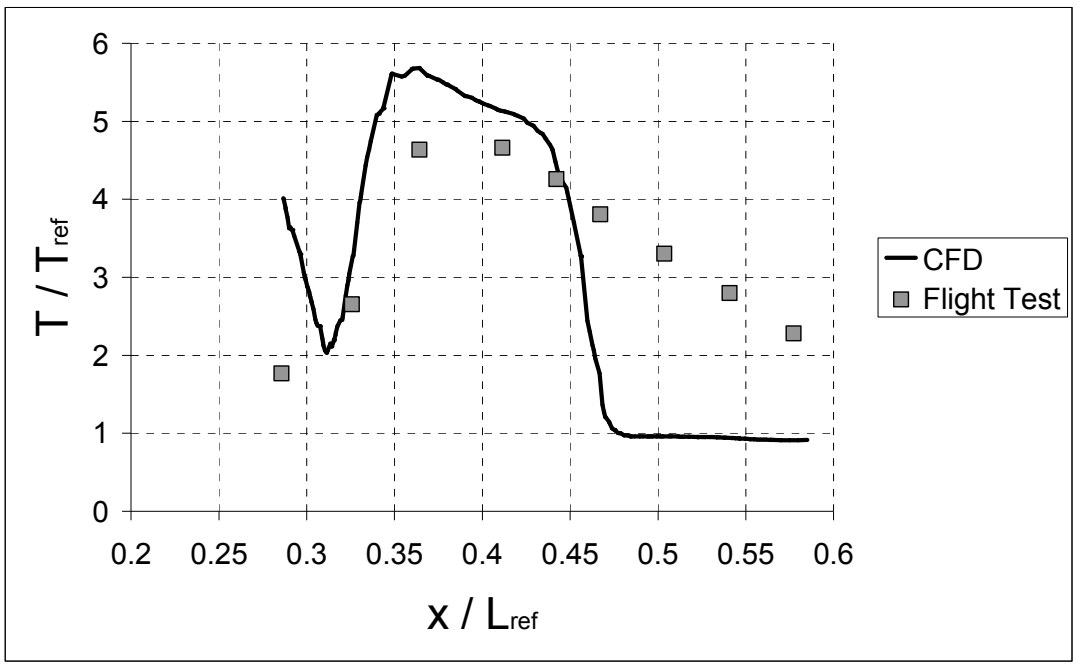

Figure 19 – *Temperature values along the upper right data line at μ=0.07*

On the lower right side (Figure 20), the numerical solution underestimates the temperature values, especially on the rear part of the tail boom. On the left side, the wake of the store hits the tail boom and creates a hot spot there (Figure 18). The temperature distributions on this side of the tail boom are strongly affected by the stores (Figure 21 and Figure 22).

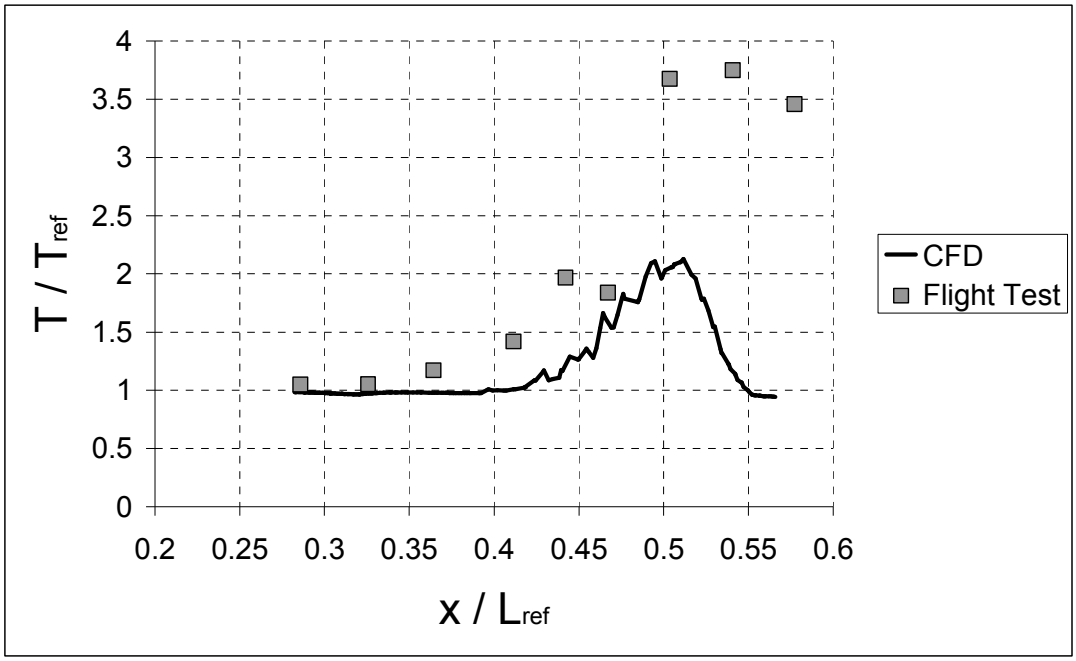

Figure 20 – *Temperature values along the lower right data line at μ=0.07*

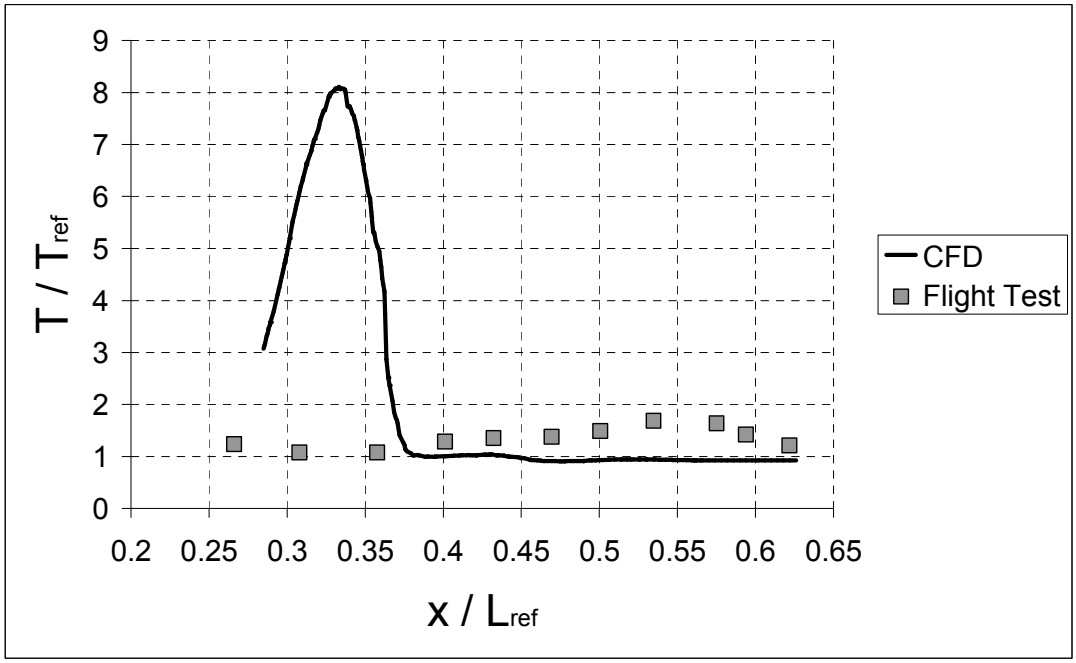

Figure 21 – *Temperature values along the upper left data line at μ=0.07*

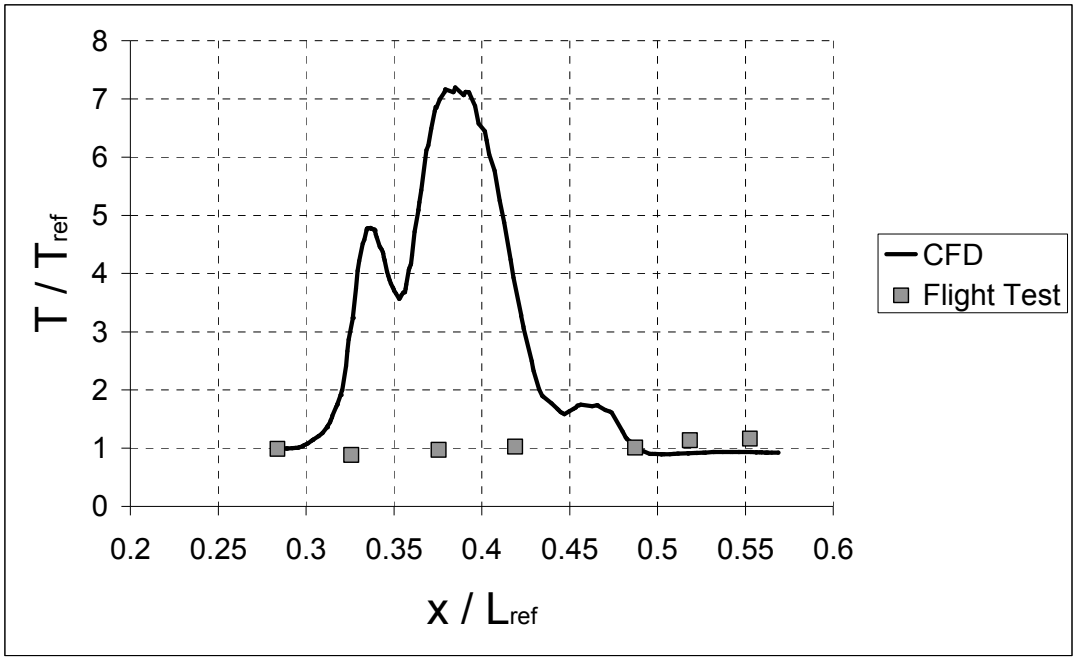

Figure 22 – *Temperature values along the lower left data line at μ=0.07*

The temperature distributions obtained from the CFD simulations at μ=0.07 are in less accord with the flight test data compared to high advance ratio simulations. With decreased flight velocity, the rotor downwash is more influent in the flow field, causing stronger unsteady effects up on the tail boom. This difference is attributed mainly to time-averaged nature of the Virtual Blade Model and the steady-state CFD approach.

CONCLUSION

In this study, the flow field of a utility helicopter in forward flight including the thermal effects of engine exhaust gases is investigated. The engine effects are included in the simulations as boundary conditions. The rotors are modeled using the Virtual Blade Model. The temperature distributions around the tail boom are compared to flight test data.

It is observed that the CFD simulations capture the general features of the helicopter flow field reasonably well. Trendwise, the simulation results and the test data show reasonably good agreement. However, in general, the temperature values are overestimated by the numerical solution.

The differences between the numerical results and the flight test data can be attributed to the approach used in the calculation of the exhaust temperatures, the rough modeling of the stores, and atmospheric disturbances as well as to some extent the steady state approach used in the numerical study.

The study shows that, CFD can provide important information during design and modification phases of helicopters. Though the need for tests cannot totally be eliminated, this information can also be utilized for the planning of the flight tests.

References

[1] Pekel Y., Trajectory Computation of Small Solid Particles Released and Carried by Flowfields of Helicopters in Forward Flight, M.S. Thesis, METU, January 2010

[2] Caliskan S., Development of Forward Flight Trim and Longitudinal Dynamic Stability Codes and Their Application to a UH-60 Helicopter, M.S. Thesis, METU, February 2009

[3] Fluent 6.3 Documentation: User's Guide, UDF Manual, Fluent, Inc., 2006

[4] Ruith M, Unstructured, Multiplex Rotor Source Model With Thrust And Moment Trimming - Fluent's VBM Model, 23rd AIAA Applied Aerodynamics Conference, AIAA 2005-5217, 2005

[5] Leishman, J., Principles of Helicopter Aerodynamics, Cambridge University Press, 2002

[6] Ballin M, A High Fidelity Real-Time Simulation of a Small Turboshaft Engine, NASA Technical Memorandum, NASA-TM-100991, 1988